

**Morphine induces redox-based changes in global DNA methylation and retrotransposon
transcription by inhibition of EAAT3-mediated cysteine uptake**

Malav Trivedi, Jayni Shah, Nathaniel Hodgson, Byun Hyang-Min and Richard Deth.

Department of Pharmaceutical Sciences, Northeastern University, Boston, MA 02115, USA -
MT, JS, NH, RD

Center for Molecular Biology and Biotechnology, Florida Atlantic University, Jupiter, FL-
33458, USA – RD.

Department of Environmental Epidemiology, Harvard School of Public Health, Boston, MA
02115, USA - BHM

Running title: Morphine induced epigenetic changes via EAAT3.

Corresponding author:

Richard C. Deth
Northeastern University 140 The Fenway
360 Huntington Avenue
Boston, MA 02115
Telephone: 617-373-4064
FAX: 617-373-8886
Email: r.deth@neu.edu

Text pages: 45.

Number of tables: 0 (main text) + 3 (supplemental).

Number of figures: 7.

Total number of References: 60.

Word count- Abstract: 250

- **Introduction:** 729.

-**Discussion:** 1422.

List of Abbreviations

DNMT: DNA methyl transferase enzyme
EAAT3: excitatory amino acid transporter type 3
ERK2: extracellular signal-regulated kinase 2
GSH: reduced glutathione
GSSG: oxidized glutathione
GTRAP3-18: glutamate transporter EAAC1-associated protein
HCY: homocysteine
JNK: c-Jun N-terminal kinase
LINE1-long interspersed nuclear elements
MAPK: mitogen-activated protein kinase
MeDIP: methylated DNA immunoprecipitation
MOR: μ opioid receptor
MS: methionine synthase
PI3K: phosphatidylinositol 3-kinase
PKA: protein kinase A
ROS: reactive oxygen species
SAM: S-adenosylmethionine
SAH: S-adenosylhomocysteine

Abstract

Canonically, opioids influence cells by binding to a G protein-coupled opioid receptor (GPCR), initiating intracellular signaling cascades such as protein kinase (PKA) (Bernstein and Welch, 1998), phosphoinositide-3 kinase (PI3K) (Yin et al., 2006), and extracellular receptor kinase (ERK) pathways (Muller and Unterwald, 2004). This results in several downstream effects, including decreased levels of the reduced-form of glutathione (GSH) and elevated oxidative stress (Goudas et al., 1999), as well as epigenetic changes, especially in retrotransposons and heterochromatin (Sun et al., 2012), although the mechanism and consequences of these actions are unclear. We characterized the acute and long-term influence of morphine on redox and methylation status (including DNA methylation levels) in cultured neuronal SH-SY5Y cells. Acting via μ opioid receptors (MORs), morphine inhibits EAAT3-mediated cysteine uptake via multiple signaling pathways, involving different G-proteins and protein kinases in a temporal manner. Decreased cysteine uptake was associated with decreases in both the redox and methylation status of neuronal cells, as defined by the ratios of reduced (GSH) to oxidized (GSSG) forms of glutathione and S-adenosylmethionine (SAM) to S-adenosylhomocysteine (SAH) levels, respectively. Further, morphine induced global DNA methylation changes, including CpG sites in LINE-1 retrotransposons, resulting in increased LINE-1 mRNA. Together, these findings illuminate the mechanism by which morphine, and potentially other opioids, can influence neuronal-cell redox and methylation status including DNA methylation. Since epigenetic changes are implicated in drug addiction and tolerance phenomenon (Renthal and Nestler, 2008), this study could potentially extrapolate to elucidate a novel mechanism for action of other drugs of abuse.

Introduction

Opioids, as exemplified by morphine, are a primary option for managing acute and chronic pain, but development of tolerance and addiction is a major problem. Specific downstream signaling cascades of MOR have been documented to contribute towards development of morphine tolerance (Bernstein and Welch, 1998; Christie, 2008). Similarly, opioid-induced oxidative stress and decreased levels of the antioxidant GSH are also suggested to contribute to opioid addiction (Xu et al., 2006); however, the mechanism through which morphine promotes oxidative stress is unclear. Moreover, the sequence of events by which morphine-induced oxidative stress might contribute to development of tolerance and opioid addiction is poorly characterized.

GSH is the major intracellular antioxidant throughout the body, and it is especially critical in the brain, due to a high rate of aerobic metabolism (Aoyama et al., 2008; Rose et al., 2012). Despite this, neuronal concentrations of GSH are lower than other cell types (Aoyama et al., 2006), allowing minor fluctuations in GSH homeostasis to readily induce oxidative stress-related neuronal damage (Aoyama et al., 2006). As in other cells, cysteine is the rate-limiting precursor for neuronal GSH synthesis (Aoyama et al., 2008); however, unlike other cells in the brain which take up cystine and reduce it to cysteine for GSH synthesis, neurons primarily depend upon uptake of extracellular cysteine, which is derived from GSH exported by astrocytes (Aoyama et al., 2008).

Excitatory amino acid transporter type 3 (EAAT3), also known as EAAC1, provides the primary route of cysteine uptake by neurons, and a knockout of EAAT3 leads to significantly reduced neuronal GSH levels and neurodegeneration (Aoyama et al., 2006; Chen and Swanson, 2003; Himi et al., 2003). Under basal conditions, EAAT3 is primarily sequestered in intracellular

vesicles, with only about 20% of the transporter being localized at the cell surface. Several factors, e.g. glutamate transporter regulator 3-18 (GTRAP3-18), growth factors and PKC regulate trafficking of EAAT3 to the cell surface (Himi et al., 2003; Nieoullon et al., 2006; Watabe et al., 2008).

A second source of intracellular cysteine for GSH synthesis is provided by transsulfuration of homocysteine (HCY), a product of the methionine cycle of methylation. However, in neurons this pathway is only a minor contributor to GSH synthesis, due to lower activity of cystathionine-gamma-lyase (Aoyama et al., 2008), as illustrated in Fig. 1. Alternatively, HCY can be converted to methionine via the activity of methionine synthase (MS), and MS activity is dependent upon the GSH-based redox status of the cell (Waly et al., 2011). Methionine is a precursor for SAM, which donates methyl groups for more than 250 methylation reactions, and is subsequently converted to SAH upon methyl group donation (Cheng and Blumenthal, 1999). SAH is reversibly converted to HCY and, since SAH accumulation can inhibit methyltransferase reactions, MS activity and the relative levels of SAM and SAH dictate the intracellular methylation potential, further affecting protein, RNA (Trivedi and Deth, 2012), DNA and histone methylation (Chiang et al., 1996). Thus, redox status regulates methylation status in neurons, through the intermediate involvement of MS.

Chronic morphine administration down-regulates spinal EAAT3 levels via PKA-dependent induction of its ubiquitin/proteasome-mediated degradation (Mao et al., 2002; Yang et al., 2008), and it has been proposed that this morphine-induced decline in cell-surface EAAT3 expression might contribute to development of morphine tolerance (Mao et al., 2002) and associated withdrawal symptoms (Xu et al., 2003). Additionally, morphine-induced condition

place preference (CPP) is shown to be associated with decreased EAAT3 expression in hippocampus (Liu et al., 2011). However, the effect of morphine on EAAT3-mediated cysteine transport and GSH status in neuronal cells has not been characterized. In this study, we investigated the effects of morphine on EAAT3-mediated cysteine uptake in SH-SY5Y neuroblastoma cells, and assessed its subsequent impact on intracellular levels of GSH and GSSG.

Epigenetic changes, including changes in both DNA and histone methylation, have recently been reported in nucleus accumbens and other brain regions following morphine administration (Maze and Nestler, 2011; Sun et al., 2012). Since DNA methylation is dependent upon SAM and SAH levels, we investigated whether morphine-induced changes in GSH/GSSG and SAM/SAH are translated into changes in global DNA methylation levels. Lastly, morphine-induced changes in epigenetic regulation of repetitive elements, especially LINE-1 retrotransposons, have also been recently reported (Sun et al., 2012). Thus, we also investigated the effect of morphine treatment on the methylation status of CpG sites in LINE-1 retrotransposon and the consequential changes in LINE-1 transcript levels.

Materials and Methods

Materials

Minimum essential medium, alpha-modification (α -MEM), trypsin, Hank's balanced salt solution (HBSS) and penicillin/streptomycin antibiotic solution were purchased from Mediatech (Manassas, VA). Fetal bovine serum (FBS) was obtained from Hyclone (Logan, UT). [35 S]-cysteine was purchased from American Radiolabeled Chemicals (St. Louis, MO). SH-SY5Y human neuroblastoma cells were purchased from ATCC[®] (Manassas, VA).

Cell Culture

Cells were grown as monolayers in 10 cm tissue culture dishes, containing 10 mL of alpha-modified Minimum Essential Medium (α -MEM) supplemented with 1% penicillin-streptomycin-fungizone (antibiotics) and 10% fetal bovine serum (FBS), in an incubator chamber with 5% CO₂ at 37°C. For most experiments, cells were plated and incubated for 48 hours prior to use.

Cysteine Uptake

Cysteine uptake was evaluated using the method developed by Chen and Swanson (Chen and Swanson, 2003). In brief, SH-SY5Y human neuroblastoma cells were plated in six-well standard tissue culture plates containing 2 mL of media for 48 hours before the assay. Confluent cells were then pretreated and incubated for various time-points prior to measuring uptake. Media was aspirated after pretreatment and cells were washed with 600 μ L of 37°C Hanks Buffered Salt Solution (HBSS). Non-radioactive HBSS was aspirated, replaced with 600 μ L of 37°C HBSS containing radiolabeled cysteine ([35 S]cysteine, (1 μ Ci/ mL)), 10 μ M unlabeled cysteine and 100

μM DTT, and incubated for 5 minutes. The [^{35}S]cysteine/HBSS mixture was aspirated and treatment was terminated with 2X washes of ice-cold HBSS. Cells were then lysed with 600 μL of dH_2O , scraped, collected in 1.5 mL microcentrifuge tubes, and sonicated for 10 seconds. 100 μL of each sample was aliquoted for a Lowry protein assay. 200 μL of each sample (in triplicate) was aliquoted into scintillation vials with 4 mL of scintillation fluid, vortexed, and counted for radioactivity. Samples were normalized against protein content. Protein concentration was determined by the modified Lowry method for protein quantification using bovine serum albumin (BSA) as the standard.

Isolation of intracellular thiol metabolites:

SH-SY5Y neuroblastoma cells were grown to confluence in α -MEM as above, and morphine or other drugs were added for specified periods of time, similar to cysteine uptake studies. Media was aspirated and the cells were washed 2X with 1 mL of ice cold HBSS. HBSS was aspirated and 0.6 mL ice cold dH_2O was added to the cells. Cells were scraped from the flask/dish and suspended in the dH_2O . The cell suspension was sonicated for 15 seconds on ice and 100 μL of sonicate was used to determine protein content. The remaining lysate was added to a microcentrifuge tube and an equal volume of 0.4 N perchloric acid was added, followed by incubation on ice for 5 min. Samples were centrifuged at 13,000 RPM and the supernatant transferred to new microcentrifuge tubes. 100 μL of sample was added to a conical microautosampler vial and kept at 4°C in the autosampler cooling tray. 10 μL of this sample was injected into the HPLC system.

HPLC measurement of intracellular thiols:

The separation of redox and methylation pathway metabolites was accomplished using an Agilent Eclipse XDB-C8 analytical column (3 x 150 mm; 3.5 μ m) and an Agilent Eclipse XDB-C8 (4.6 x 12.5 mm; 5 μ m) guard column. Two mobile phases were used: Mobile Phase A was 0% acetonitrile, 25 mM sodium phosphate, 1.4 mM 1-octanesulfonic acid, adjusted to pH 2.65 with phosphoric acid. Mobile Phase B was 50% acetonitrile. The flow rate was initially set at 0.6 mL/min and a step gradient was utilized: 0-9 min 0% B, 9-19 min 50% B, 19-30 min 50% B. The column was then equilibrated with 5% B for 12min prior to the next run. Temperature was maintained at 27 °C. The electrochemical detector was an ESA CoulArray with BDD Analytical cell Model 5040 and the operating potential was set at 1500 mV. Sample concentrations were determined from the peak areas of metabolites using standard calibration curves and ESA-supplied HPLC software. Sample concentrations were normalized against protein content. In some cases samples were diluted in mobile phase as needed or up to 50 μ L of sample were injected to assure that thiol levels were within the range of the standard curve.

DNA Isolation

DNA from cultured cells after appropriate treatment for the analysis of DNA methylation was harvested and isolated as previously described (Hodgson et al., 2013) using the FitAmpTM Blood & Cultured Cell DNA Extraction Kit from Epigentek[®]. The full protocol can be obtained from the manufacturer's website. Isolated DNA was quantified using a ND-1000 NanoDrop spectrophotometer.

DNA Methylation Analysis

DNA was isolated from SH-SY5Y cell culture after various pretreatments and any contaminating RNA was removed by RNAase treatment. Assessment of global DNA methylation status was accomplished as described previously (Hodgson et al., 2013) using the MethylFlash® Methylated DNA Quantification Kit from EPIGENTEK® (See manufacturer's website for full protocol). The methylated fraction of DNA was identified using 5-methylcytosine monoclonal antibodies and quantified by an ELISA-like reaction. The levels of methylated DNA were calculated using the OD intensity on a microplate reader at 450 nm.

Genome wide CpG methylation: Fragmentation and MBD-capture

Genomic DNA was extracted from samples with the Easy DNA kit (Invitrogen K1800-01) using the appropriate protocol for cell lines. For a full overview of the MethylCap-Seq protocol, refer to (De Meyer et al., 2013). In summary, fragmentation was performed with a Covaris S2 with the following settings: duty cycle 10%, intensity 5, 200 cycles per burst during 200 sec, to obtain fragments with an average length of 200 bp. The power mode was frequency sweeping, temperature 6-8° C, water level 12. A maximum of 5 µg was loaded in 130 µL Tris-EDTA in a microtube with adaptive focused acoustics (AFA) intensifier. For samples with less DNA input (down to 500 ng) we diluted the DNA in 1:5 diluted TE. DNA with an input from 5- 3 µg was analyzed on the Agilent 2100 on a DNA 1000 chip. DNA with an input lower than 3 µg was concentrated in a rotary evaporator to 25 µL and the fragment distribution checked on a high sensitivity DNA chip. Methylated DNA was captured using the MethylCap kit (Diagenode, Belgium), according to the manufacturer's protocol; starting concentration was 200 ng. The yield was typically between 0.5 and 8 ng total captured DNA. Fragments were subsequently

sequenced using the Illumina Genome Analyzer II. The concentrations of the fragmented and captured DNA was determined on a Fluostar Optima plate reader with the Quant-iT PicoGreen dsDNA Assay Kit (Invitrogen P7589) at 480/520nm.

To prepare the DNA library we used the DNA Sample Prep Master Mix Set 1 (NEB E6040) in combination with the Multiplexing Sample Preparation Oligo Kit (96 samples, Illumina PE-400-1001). We use the entire fragmented DNA and followed the NEB protocols. NEBNext End Repair Module Protocol: Purify with a Qiaquick PCR Purification Kit (Qiagen 28104) and elute in 37 μ L Elution Buffer (EB). NEBNext dA-tailing Module Protocol: Purify on a Minelute PCR Purification Kit (Qiagen 28004) and elute in 25 μ L EB. NEBNext Quick Ligation Module Protocol: Purify on a Minelute PCR Purification Kit (Qiagen 28004) and elute in 30 μ L EB, using the multiplexing sequencing adapters provided in the Multiplexing Sample Preparation Oligo Kit. Size selection of the library was done on a 2% agarose gel (Low Range Ultra Agarose Biorad 161-3107). We used a 1Kb Plus ladder (Invitrogen 10787-018) and ran the gel at 120 V for 2 hrs. A fragment of 300 bps +/- 50bps was excised and eluted on a Qiagen Gel Extraction Kit column (Qiagen 28704) and eluted in 23 μ L EB.

We followed the Illumina library amplification index protocol with the following alterations: We used 22 μ L DNA and performed 21 cycles. The sample was purified on a Qiaquick PCR Purification column (Qiagen 28101) and eluted in 50 μ L EB, 1:5 diluted, concentrate in a rotary evaporator to 10 μ L and 1 μ L was applied to a Agilent 2100 HS DNA chip and the concentration was determined by smear analysis on the Agilent 2100. The samples were diluted to 10 nM. After denaturation with NaOH we diluted the samples to 16 pM. The Paired-End flow cell was prepared according to the Cluster Station User Guide. Sequencing was performed according to

the HiSeq user guide (performing a Multiplexed PE Run), with 2 x 51 cycles for the paired end runs.

Analysis of the methylation levels in the repeat elements LINE-1

Reads from each sample were mapped onto the repeat element LINE1 sequence. All LINE-1 elements were selected by searching the RepeatMasker table (assembly of April 2003) at <http://genome.ucsc.edu> for all L1 elements. Full-length elements belonging to the LINE-1 family were then aligned to each other and mapped using low stringency settings (bowtie, single end, allowed multiple hits = 1000, mismatches in the seed = 1). The number of elements mapped and counted for each treatment datapoint can be found in Supplemental Table S3. We then evaluated the average mapped read ratios for each group vs. control and calculated a corresponding Chi-Square value and depicted them, along with the methylation ratio, which depicts the odds ratio normalizing the 5meC levels for treated groups against the control group.

Bisulfite sequencing for measuring site-specific CpG methylation in LINE1 retrotransposons

For bisulfite sequencing, DNA was isolated from SH-SY5Y cells using the FitAmpTM Blood & Cultured Cell DNA Extraction Kit from EPIGENTEK[®]. The extracted DNA (500 ng; concentration: 50 ng/mL) was treated with the EZ DNA Methylation-Gold Kit (Zymo Research, Orange, CA, USA) according to the manufacturer's protocol. 30 mL of M-Elution Buffer (Zymo Research) was used for the final elution. Methylation of DNA was quantified with bisulfite treatment of DNA and simultaneous polymerase chain reaction (PCR) followed by pyrosequencing, using primers and conditions previously described.(Alexeeff et al., 2013) A 50-

μL PCR was performed in 25 μL of GoTaq Green Master mix (Promega, Madison, WI, USA), with 1pmol biotinylated forward primer, 1 pmol reverse primer, 50 ng bisulfite-treated genomic DNA, and water. Results were reported as the percent of the sum total of methylated and unmethylated cytosines that consisted of 5-methylated cytosines (%5mC). Additionally, non-CpG cytosine residues were used as internal controls to validate bisulfite conversion. The pyrosequencing-based assay can evaluate individual measures of methylation at more than one CpG dinucleotide. All samples were subjected to a quality control check incorporated in the software which evaluates the bisulfite conversion rate of any cytosine not followed by a guanine. LINE-1 Methylation levels were analyzed at four different CpG sites. The primer sequences is provided in Supplementary Table S2.

RNA Isolation

Cells were maintained and plated in six-well culture dishes as described above. After appropriate treatments, RNA was isolated as described previously (Hodgson et al., 2013) using the RNAqueous®-4PCR kit from Ambion®. For a full protocol please refer to the manufacturer's protocol. The isolated RNA was treated with DNase, as stated in the extended RNA isolation protocol, followed by RNA quantification using a ND-1000 NanoDrop spectrophotometer.

Primers

All custom primers were designed using the Invitrogen OligoPerfect™ Designer to have between 50-60% GC content, an annealing temperature of 60°C and a length of 20 bases. Primer sets were checked for primer-dimer formation and each primer was specific for the desired template. Full primer sequences can be found in Supplementary Table 2. GAPDH primers were uniform in

expression and validated in qRT-PCR studies; therefore, the housekeeping gene GAPDH was an appropriate internal and loading control.

cDNA synthesis

cDNA synthesis and subsequent PCR amplification were performed using the First strand cDNA synthesisTM from Roche. The cDNA synthesis uses 1 µg RNA, 1 mM dNTP mix, 60 µM random hexamer primers, with sufficient molecular biology grade H₂O added to achieve a final sample volume of 13 µL. Samples were denatured at 65°C for 5 minutes and then placed on ice. Transcriptor RTTM (20 units/µL), Protector RNase inhibitorTM (40 U/µL), 5x Transcriptor Reverse Transcriptase Reaction Buffer and molecular biology grade H₂O in a final volume of 7 µL were used in the second part of the reaction to bring the final volume to 20 µL. This was followed by incubation in the PTC-Thermocycler (MJ Research) at 25°C for 10 min followed by 30 min at 55°C. The reverse transcriptase enzyme was inhibited by incubation at 85°C for 5 min.

qRT-PCR Analysis

qRT-PCR was performed on triplicate samples using the LightCycler® 480 qRT-PCR machine from RocheTM as described previously (Hodgson et al., 2013). The assay was run in 96-well optical reaction plates. qRT-PCR uses 5 µL of cDNA template, 10 µM sense and antisense primers, 10 µL SYBR Green I Master® from RocheTM, and dH₂O in a final volume of 20 µL. The following thermal parameters will be used: incubation for 5 min at 95 °C, and then 45 cycles of 95 °C for 10 sec, 60 °C for 20 sec and 72 °C for 30 sec, followed by a single cycle of 95 °C for 5 sec, 1 min at 65 °C and 97 °C for the melting curve, followed by cooling at 40 °C for 90 sec. No template controls were run on each plate, and dissociation curves were generated to

determine any non-specific products. Data were analyzed using the Roche quantification method $\Delta(\Delta C_t)$ and were normalized to GAPDH levels.

Statistical Methods

Graph Pad Prism[®] version 5.01 was used for all statistical analyses. Student's t-test was used for independent means to test for significant differences between control and experimental groups. Data were expressed as mean \pm standard error of the mean (SEM). Non-linear and linear regression models were used to calculate the best-fit values. Non-linear regressions used a two-phase exponential decay function. Comparisons between multiple groups of data were conducted using one-way analysis of variance (ANOVA), and Turkey's post-hoc test was used to determine the differences between individual groups

Results:

Morphine inhibits EAAT3 mediated cysteine transport via the μ opioid receptor.

As noted earlier, cysteine is the rate-limiting precursor for synthesis of GSH, and EAAT3 accounts for 90% of cysteine uptake in neuronal cells, making it a key regulator of GSH synthesis (Chen and Swanson, 2003). We previously reported the prominent expression of EAAT3 in SH-SY5Y neuroblastoma cells, as compared to other EAAT family members, and we also showed that EAAT3 is the major route of cysteine transport in this cell line (Hodgson et al., 2013). To investigate the effects of morphine on EAAT3 mediated cysteine uptake, we treated SH-SY5Y cells with graded concentrations of morphine (0.1 nM – 10 μ M) for 30 minutes and measured [³⁵S]-radiolabeled cysteine uptake. Morphine inhibited [³⁵S]-radiolabeled cysteine transport in a dose-dependent manner, with an IC₅₀ of 2.4 nM (Fig. 2A). Pre-treatment with naltrexone (a non-selective opioid antagonist) blocked morphine inhibition of [³⁵S]-cysteine uptake, indicating opioid receptor involvement in mediating its inhibition of EAAT3 activity (Fig. 2A).

Since SH-SY5Y cells express both μ - and δ -opioid receptors (Daijo et al., 2011), we wanted to identify the specific opioid receptor subtype involved in mediating morphine effects on EAAT3. Accordingly, we pretreated SH-SY5Y cells with either the μ -opioid receptor-specific antagonist D-Phe-Cys-Tyr-D-Trp-Arg-Thr-Pen-Thr-NH₂ (CTAP), or the δ -opioid receptor specific antagonist naltrindole (NTI), prior to treatment with morphine (0.1 μ M) for different time intervals. As shown in Fig. 2B, pre-treatment with CTAP (0.1 μ M), blocked the short-term (0.5 and 4 hours), as well as long-term (24 hours) effects of morphine, whereas NTI (0.1 μ M) had no

effect on morphine-induced inhibition of cysteine transport at any time-point. Hence, μ -opioid receptor activation mediates the ability of morphine to inhibit cysteine transport via EAAT3.

Next, we wanted to investigate whether the inhibitory effect of morphine on cysteine uptake alters intracellular levels of cysteine, GSH or GSSG and/or affects cellular redox status. Additionally, since redox status can affect SAM levels, we also measured intracellular SAM and SAH levels, as well as other thiol containing metabolites. For this purpose, SH-SY5Y cells were treated with morphine (0.1 μ M) for different time intervals, and cellular thiol and thiol-ether metabolites, including GSH, oxidized GSH, SAM and SAH, were measured via HPLC with electrochemical detection. Morphine significantly decreased cellular levels of cysteine, as well as GSH/GSSG and SAM/SAH ratios, the latter being indicators of oxidative stress and methylation capacity, respectively (Fig. 4 and Supplementary Table S1). Together these results demonstrate the ability of morphine to influence both redox state and methylation capacity of neuronal cells via its inhibitory effect on EAAT3-mediated cysteine uptake.

G proteins involved in morphine-induced inhibition of EAAT3-mediated cysteine transport

Morphine has the ability to activate multiple G proteins (e.g. $G_{i/o}$ and G_s) in SH-SY5Y cells via the μ -opioid receptor (Wang et al., 2009). Hence, we wanted to characterize the specific G-proteins involved in mediating the effects of morphine on EAAT3-mediated cysteine uptake. We used pertussis toxin (PTX) and cholera toxin (CTX), to inhibit $G_{i/o}$ and G_s , respectively. As indicated in Fig. 3A, pre-treatment with PTX (0.5 μ g/mL, 24 hrs) abolished short-term (30 min and 4 hr) effects of morphine on cysteine transport, but did not alter long-term (24 hr) effects. Interestingly, pre-treatment with CTX (0.5 μ g/mL, 24 hrs) blocked the long-term effects, but did not affect the short-term effects of morphine on cysteine transport (Fig. 3A). These results

indicate that short-term effects of morphine are mediated by activation of the G_i -subtype of G proteins, coupled to the μ -opioid receptor, whereas the long-term effects involve coupling of μ -opioid receptors to G_s . Thus, different G proteins are coupled to the μ -opioid receptor in a temporal manner to induce the inhibitory effect of morphine on EAAT3 in SH-SY5Y cells.

Protein kinases involved in morphine-induced inhibition of EAAT3-mediated cysteine transport

PKA (Guillet et al., 2005; Lim et al., 2005) and ERK (Guillet et al., 2005) are involved in regulating the activity and surface expression of EAAT3 in SH-SY5Y cells. Studies also indicate differential activation of downstream protein kinases under the influence of acute vs chronic morphine (Bilecki et al., 2005; Muller and Unterwald, 2004). Hence, we wanted to identify the downstream signaling protein kinases involved in mediating the effects of morphine on EAAT3. For this purpose, we used the PKA inhibitor H-89 and the MAPK / ERK kinase inhibitor PD98059. Pre-treatment with H-89 (0.1 μ M, 4 hrs) blocked short-term effects of morphine, whereas, pre-treatment with PD98059 (10 μ M, 24 hrs) blocked long-term effects of morphine (Fig. 3B). These results indicate that PKA is involved in mediating the short-term effects of morphine and MAPK/ERK kinase is involved in mediating the long-term effects of morphine. Pre-treatment with protein kinase inhibitors H-89 (0.1 μ M, 4 hrs) and PD98059 (10 μ M, 24 hrs), also blocked short-term and long-term effects of morphine on cellular levels of cysteine, respectively (Fig. 4, Table S1), and subsequent changes in GSH/GSSG and SAM/SAH ratios were also blocked (Fig. 4, Table S1). These results support previous studies indicating that PKA and MAPK/ERK kinase are involved in mediating the acute and chronic effects of morphine (Guillet et al., 2005; Lim et al., 2005; Muller and Unterwald, 2004).

Long-term but not short-term morphine treatment induces DNA hypomethylation.

Morphine was recently shown to decrease histone methylation levels in nucleus accumbens of rodent brain (Sun et al., 2012), but the ability of morphine to affect DNA methylation has as yet not been characterized. Hence, we wanted to investigate if morphine-induced changes in SAM/SAH would affect the methylation activity in the neuronal cells, especially DNA methylation. Global DNA methylation levels were measured using anti-5-methylcytosine monoclonal antibodies, quantified by an ELISA-like reaction. As indicated in Fig. 5, global DNA methylation decreased significantly after long-term treatment with morphine, and this effect was blocked by pre-treatment with PD-98059 (10 μ M, 24 hrs); however, short-term treatment of morphine did not alter global DNA methylation. These changes in global DNA methylation levels correspond with changes in the levels of SAM/SAH under the influence of morphine (Fig. 4), and they indicate that morphine affects DNA methylation via a redox-regulated methylation pathway, which is a consequence of changes in EAAT3-mediated cysteine transport. Previously, we showed that a specific EAAT3 blocker (L-beta-threo-benzylaspartate; LBTBA) can inhibit cysteine uptake and induce changes in intracellular thiol and thiol ether metabolites and these changes were translated further to decreased GSH/GSSG and SAM/SAH ratios (Hodgson et al., 2013). Furthermore, LBTBA also induced global DNA hypomethylation (Hodgson et al., 2013). Hence, the effects of morphine are similar to a specific inhibitor of EAAT3, indicating that EAAT3-mediated cysteine uptake is a key regulator of redox status and DNA methylation levels.

Morphine alters DNA methylation in repetitive elements

Long interspersed nuclear elements (LINE-1) are the most widespread class of retrotransposons in mammals, constituting about 20% of mammalian genomic DNA (Lander et al., 2001), and the methylation status of LINE-1 retrotransposons is used as a proxy for global DNA methylation (Ohka et al., 2011). A recent study found altered histone methylation levels across several different classes of LINE-1 retrotransposons under the influence of morphine injected into the nucleus accumbens of mice (Sun et al., 2012). Studies have also demonstrated mobilization, integration and regulation of LINE-1 in several brain regions, although the functional implications remain unclear (Luning Prak and Kazazian, 2000; Singer et al., 2010). Since the influence of morphine on LINE-1 DNA methylation has not as yet been characterized, we investigated the effects of short-term and long-term morphine treatment on LINE-1 methylation status in SH-SY5Y cells using MBD sequencing. We also wanted to investigate whether the changes in LINE-1 methylation levels followed similar pattern as observed with global DNA methylation levels. Long-term (24 hr) treatment with morphine induced hypomethylation of CpG sites across entire LINE-1 regions, whereas short-term (4 hr) treatment induced CpG hypermethylation (Supplementary Table S3). The results correlate with temporal changes in the levels of SAM/SAH (Fig. 4), as well as with changes in global DNA methylation under the influence of morphine (Fig. 5). However, when we characterized site-specific methylation at four individual CpG sites in the promoter region of LINE-1Hs (human lineage specific) family after morphine treatment using bisulfite treatment followed by pyrosequencing, we found different results. As shown in Fig. 6A, the CpG site at position 3 is hypomethylated after morphine treatment for 4 hours and 24 hours of morphine exposure. However, at position 4,

methylation was increased after 24 hours of morphine treatment, but not after 4 hours morphine. Hence, different CpG sites in LINE1 exhibit temporally differential methylation in response to morphine treatment.

To further characterize overall changes in the promoter region, we evaluated CpG methylation levels near the transcription start site of LINE-1 (TSS \pm 500 base pairs) under the influence of morphine at 4 and 24 hrs using MBD sequencing. Fig. 6B illustrates a significant shift to hypermethylation in the promoter region under the influence of short-term treatment with morphine, but a return to control methylation levels after long-term morphine treatment.

To determine whether morphine-induced changes in LINE-1 CpG methylation were associated with changes in its transcription, we designed primers specific for the LINE1-Hs (human-lineage specific) family and quantified the respective mRNA levels using qRT-PCR. Short-term treatment with morphine significantly decreased LINE-1 mRNA levels (Fig. 6B), which corresponds to increased CpG methylation levels in the promoter regions of LINE-1 following short-term morphine treatment (Fig. 6B). Long-term treatment with morphine induced a significant elevation of LINE-1 mRNA levels, consistent with the decreased LINE-1 promoter methylation (Fig. 6B). Taken together, these results indicate that morphine-induced changes in cysteine transport modulate the intracellular levels of cysteine, alter cellular redox and methylation status (Supplementary Table S1, Fig. 4), and subsequently induce changes in global changes in methylation, including global DNA methylation, reflected as time-dependent changes in the transcription of LINE-1 retrotransposons (Fig. 6).

Discussion:

While the pharmacological actions of morphine are among the most extensively studied of any drug, significant gaps remain in our understanding of the molecular mechanisms involved in its provision of pain relief and euphoria, as well as its propensity for tolerance and addiction. Morphine-induced activation of multiple G protein signaling pathways via μ - and δ -opioid receptors has been well-documented (Wang et al., 2009), and effects via non-G protein signaling pathways such as toll-like receptor activation are also known (Hutchinson et al., 2012). The current studies reveal an ability of morphine to modulate uptake of cysteine in cultured human neuronal cells via MOR activation, initiating a pathway of metabolic effects resulting in altered redox and methylation status, including changes in global DNA methylation and gene transcription. Together these actions constitute a novel signaling mechanism affecting a large number of redox and methylation-sensitive cellular processes with particular significance for the development of addiction.

Previous *in vitro* studies report downregulation of EAAT3 under morphine exposure followed by recovery upon morphine withdrawal (Mao et al., 2002; Yang et al., 2008). Morphine-induced condition place preference leads to decreased EAAT3 expression in hippocampus (Liu et al., 2011). We observed both short and longer-term inhibitory effects of morphine on EAAT3-mediated cysteine uptake in SH-SY5Y cells involving MOR-mediated activation of different G proteins. Short-term (0.5 and 4 hr) inhibition involved activation of PTX-sensitive G proteins (e.g. G_i or G_o), while longer-term inhibition involved CTX-sensitive G proteins (e.g. G_s). Temporal differences in G protein activation may indicate progressive cellular adaptive mechanisms during continuous morphine exposure. This temporal G protein selectivity might

result from differential phosphorylation of the MOR during acute vs chronic morphine exposure, permitting selectivity for downstream signaling pathways. Indeed, adaptive changes observed at the level of G protein involvement were further translated into differential activation of downstream protein kinases. Morphine-mediated short-term inhibition was sensitive to the PKA inhibitor H-89, while longer-term inhibition was blocked by pretreatment with the ERK pathway inhibitor PD-98059. By inducing differential phosphorylation of EAAT3, protein kinases can affect cell-surface expression, or altering EAAT3 transcription, as has been described for PKC, PKA and PI3K (Guillet et al., 2005; Lim et al., 2008), which could be responsible for the observed inhibitory effects of morphine. Thus, distinctly different signaling pathways emanating from the μ -opioid receptor provide control over cysteine uptake during a 24 hr interval of exposure to morphine, which could be considered as functional selectivity at the levels of G proteins and downstream signaling molecules. This functional selectivity would be important for maintaining neuronal cell physiological balance, including redox-based epigenetic homeostasis under continuous morphine exposure

To explore the functional significance of a morphine-induced decrease in cysteine uptake, we measured the levels of thiol-containing redox and methylation pathway metabolites, and found significant reductions in both GSH/GSSG and SAM/SAH ratios, indicative of increased oxidative stress and decreased methylation capacity. This reflects the dependence of GSH synthesis on cytoplasmic cysteine levels and the sensitivity of methionine synthase to cellular redox status (Muratore et al., 2013), and provide a novel signaling pathway with exceptionally broad influence. Thus, an oxidative shift in redox status will affect a vast number of cellular processes, for example by virtue of its impact on thiol-regulated proteins (Moran et al., 2001), as

well as ROS formation and inactivation (Powis et al., 1995, 1996), while decreased methylation capacity will affect hundreds of methylation reactions including DNA methylation (Chiang et al., 1996; Schubert et al., 2003).

Epigenetic changes, specifically alterations in DNA methylation, influence learning and memory (Levenson and Sweatt, 2005; Miller et al., 2008), and opioids such as morphine can induce epigenetic changes, producing long-lasting alterations in gene expression and behavior in mice (Maze and Nestler, 2011; Sun et al., 2012). By altering cysteine uptake and redox status, morphine can exert global influence over DNA methylation, secondary to the influence of SAM/SAH on methylation of cytosine in the context of individual CpG sites or clustered CpG islands. Prior studies show changes in global DNA methylation in response to changes in MS activity (Ulrey et al., 2005; Waly et al., 2004), including an increase in response to insulin-like growth factor 1 (IGF-1)(Waly et al., 2004), and a decrease in response to oligomers of beta amyloid (Hodgson et al., 2013), associated with reciprocal increases and decreases in GSH/GSSG and SAM/SAH. We observed a significant decrease in global DNA methylation after 24 hrs of morphine treatment, corresponding to the lowest value of SAM/SAH, but not after 4 hrs. However, the LINE-1 promoter region was hypermethylated at 4 hours but returned to control levels at 24 hours. Hence, changes in global DNA methylation were not predictive of LINE-1 promoter region methylation and *vice versa*, although other regions, which might have been hypomethylated, but were not evaluated in the current study. Individual CpG regions in LINE-1 the promoter region showed lower and higher levels of methylation after 4 and 24 hrs of morphine treatment, suggesting that local factors (e.g. transcription factor occupancy, methylated CpG binding proteins) combine with broader influences (e.g. histone modifications/polycomb

group binding proteins) could produce a complex re-distribution of methylation marks in this region. The remarkable temporal pattern of changes in LINE-1 promoter region methylation in response to morphine may illustrate a general role for redox in epigenetic regulation, and future studies should provide a more detailed understanding of the underlying contributing factors.

LINE-1 mRNA transcript levels also showed morphine-induced temporal changes. Interestingly, LINE-1 promoter hypermethylation at 4 hrs correlated with decreased LINE-1 mRNA levels, however, after 24 hours LINE-1 mRNA levels were increased while LINE-1 promoter methylation levels returned to control levels. One of the possible explanation for the latter is a methylation-independent increase in cytosolic pools of LINE1 mRNA as a consequence of oxidative stress and release from secretory granules, as reported previously (Singer et al., 2010). On the other hand, individual CpG sites in the promoter region of LINE-1 could permit/hinder transcription (Deaton and Bird, 2011). Time-dependent methylation changes at Pos3 and Pos4 CpG sites in LINE-1 promoter region were observed, and CpG site Pos3 was hypomethylated at both 4 and 24 hrs under morphine exposure. However, the exact role of these changes at individual CpG sites is unclear. Decreased DNA methylation implies removal of methyl groups, and a redox-sensitive 5-hydroxymethylcytosine-directed dehydroxymethylase activity of DNMT3A and DNMT3B has been described, which is activated under more oxidized conditions (Chen et al., 2012) . Thus the morphine-induced shift in redox could also contribute to DNA hypomethylation by accelerating removal of hydroxymethyl groups. In general the actions of morphine could induce global revision of DNA methylation levels.

Epigenetic-induced changes in LINE-1 retrotransposition events (Sun et al., 2012) have been linked to drug addiction (Luning Prak and Kazazian, 2000; Maze et al., 2011). In light of the

influence of redox on methylation of DNA (and histones), the ability of morphine to modulate GSH/GSSG and SAM/SAH provides an example of how epigenetic status can be altered by drugs of abuse. Alcohol induces similar effects by lowering GSH levels and impaired methylation, (Waly et al., 2011) while cocaine (Lee et al., 2001), amphetamine (Carvalho et al., 2001) and heroin (Gutowicz et al., 2011) also alter GSH levels. While our results implicate MOR-mediated regulation of EAAT3 as the proximal event for morphine-induced changes in DNA methylation, other drugs of abuse may produce redox changes via uniquely different mechanisms. Notably, alcohol potently decreases EAAT3 activity via a protein kinase C-dependent pathway (Kim et al., 2003), and inhibits MS activity (Waly et al., 2011). Similarly, nicotine inhibits EAAT3 activity via the PKC pathway (Yoon et al., 2014). For as much as physiological factors (e.g. IGF-1) also affect EAAT3 activity, drugs of abuse can be recognized as interfering with homeostatic mechanisms that also utilize redox mechanisms to regulate gene expression via epigenetic control.

Recognition of the importance of redox and epigenetic mechanisms in addiction brings the prospect of novel targets. Use of N-acetylcysteine (NAC) in symptomatic treatment of alcohol (Ferreira Seiva et al., 2009), cocaine dependence (Mardikian et al., 2007), and withdrawal (Reichel et al., 2011) presents efforts in exploiting this pathway. EAAT3 itself may provide a potential site for pharmacologic intervention, along with factors/systems which regulate its activity. However, the use of cell cultures; SH-SY5Y cells is an important limitation of the current study and it needs to be acknowledged before any extrapolation of the current results.

In summary, we provide the first description of the ability of morphine to alter global DNA methylation and transcription of the retrotransposon LINE-1, via a novel redox-dependent

signaling mechanism initiated by μ receptor activation (Fig. 7). The functional importance of this mechanism in the actions of endogenous opioids and the multiple pharmacological actions of morphine remain to be explored.

Acknowledgments

The authors would like to thank Dr. Andrea Baccarelli (Harvard School of Public Health) for his assistance with bisulfite sequencing, and Geert Trooskens (University of Ghent) for his assistance with analysis of LINE-1 TSS methylation levels.

Authorship Contributions

Participated in research design: Trivedi, Deth.

Conducted experiments: Trivedi, Shah, Byun.

Performed data analysis: Trivedi, Shah, Hodgson, Deth.

Wrote or contributed to the writing of the manuscript: Trivedi, Deth.

References:

Alexeeff, S.E., Baccarelli, A.A., Halonen, J., Coull, B.A., Wright, R.O., Tarantini, L., Bollati, V., Sparrow, D., Vokonas, P., and Schwartz, J. (2013). Association between blood pressure and DNA methylation of retrotransposons and pro-inflammatory genes. *Int. J. Epidemiol.* *42*, 270–280.

Aoyama, K., Suh, S.W., Hamby, A.M., Liu, J., Chan, W.Y., Chen, Y., and Swanson, R.A. (2006). Neuronal glutathione deficiency and age-dependent neurodegeneration in the EAAC1 deficient mouse. *Nat. Neurosci.* *9*, 119–126.

Aoyama, K., Watabe, M., and Nakaki, T. (2008). Regulation of neuronal glutathione synthesis. *J. Pharmacol. Sci.* *108*, 227–238.

Bernstein, M.A., and Welch, S.P. (1998). μ -Opioid receptor down-regulation and cAMP-dependent protein kinase phosphorylation in a mouse model of chronic morphine tolerance. *Brain Res. Mol. Brain Res.* *55*, 237–242.

Bilecki, W., Zapart, G., Ligęza, A., Wawrzczak-Bargiela, A., Urbański, M.J., and Przewłocki, R. (2005). Regulation of the extracellular signal-regulated kinases following acute and chronic opioid treatment. *Cell. Mol. Life Sci. CMLS* *62*, 2369–2375.

Carvalho, F., Fernandes, E., Remião, F., Gomes-Da-Silva, J., Tavares, M.A., and Bastos, M.D.L. (2001). Adaptative response of antioxidant enzymes in different areas of rat brain after repeated d-amphetamine administration. *Addict. Biol.* *6*, 213–221.

Chen, Y., and Swanson, R.A. (2003). The glutamate transporters EAAT2 and EAAT3 mediate cysteine uptake in cortical neuron cultures. *J. Neurochem.* *84*, 1332–1339.

Chen, C.-C., Wang, K.-Y., and Shen, C.-K.J. (2012). The Mammalian de novo DNA Methyltransferases Dnmt3a and Dnmt3b Are Also DNA 5-Hydroxymethyl Cytosine Dehydroxymethylases. *J. Biol. Chem.* jbc.C112.406975.

Cheng, X., and Blumenthal, R. (1999). S-adenosylmethionine-dependent methyltransferases: structures and functions (World Scientific).

Chiang, P.K., Gordon, R.K., Tal, J., Zeng, G.C., Doctor, B.P., Pardhasaradhi, K., and McCann, P.P. (1996). S-Adenosylmethionine and methylation. *FASEB J. Off. Publ. Fed. Am. Soc. Exp. Biol.* *10*, 471–480.

Christie, M.J. (2008). Cellular neuroadaptations to chronic opioids: tolerance, withdrawal and addiction. *Br. J. Pharmacol.* *154*, 384–396.

Daijo, H., Kai, S., Tanaka, T., Wakamatsu, T., Kishimoto, S., Suzuki, K., Harada, H., Takabuchi, S., Adachi, T., Fukuda, K., et al. (2011). Fentanyl activates hypoxia-inducible factor 1 in neuronal SH-SY5Y cells and mice under non-hypoxic conditions in a μ -opioid receptor-dependent manner. *Eur. J. Pharmacol.* *667*, 144–152.

Deaton, A.M., and Bird, A. (2011). CpG islands and the regulation of transcription. *Genes Dev.* *25*, 1010–1022.

Ferreira Seiva, F.R., Amauchi, J.F., Ribeiro Rocha, K.K., Souza, G.A., Ebaid, G.X., Burneiko, R.M., and Novelli, E.L.B. (2009). Effects of N-acetylcysteine on alcohol abstinence and alcohol-induced adverse effects in rats. *Alcohol* 43, 127–135.

Goudas, L.C., Langlade, A., Serrie, A., Matson, W., Milbury, P., Thurel, C., Sandouk, P., and Carr, D.B. (1999). Acute decreases in cerebrospinal fluid glutathione levels after intracerebroventricular morphine for cancer pain. *Anesth. Analg.* 89, 1209–1215.

Guillet, B.A., Velly, L.J., Canolle, B., Masméjean, F.M., Nieoullon, A.L., and Pisano, P. (2005). Differential regulation by protein kinases of activity and cell surface expression of glutamate transporters in neuron-enriched cultures. *Neurochem. Int.* 46, 337–346.

Gutowicz, M., Kaźmierczak, B., and Barańczyk-Kuźma, A. (2011). The influence of heroin abuse on glutathione-dependent enzymes in human brain. *Drug Alcohol Depend.* 113, 8–12.

Himi, T., Ikeda, M., Yasuhara, T., Nishida, M., and Morita, I. (2003). Role of neuronal glutamate transporter in the cysteine uptake and intracellular glutathione levels in cultured cortical neurons. *J. Neural Transm. Vienna Austria* 1996 110, 1337–1348.

Hodgson, N., Trivedi, M., Muratore, C., Li, S., and Deth, R. (2013). Soluble Oligomers of Amyloid- β Cause Changes in Redox State, DNA Methylation, and Gene Transcription by Inhibiting EAAT3 Mediated Cysteine Uptake. *J. Alzheimers Dis. JAD.*

Hutchinson, M.R., Northcutt, A.L., Hiranita, T., Wang, X., Lewis, S.S., Thomas, J., Steeg, K. van, Kopajtic, T.A., Loram, L.C., Sfregola, C., et al. (2012). Opioid Activation of Toll-Like Receptor 4 Contributes to Drug Reinforcement. *J. Neurosci.* 32, 11187–11200.

Ikemoto, M.J., Inoue, K., Akiduki, S., Osugi, T., Imamura, T., Ishida, N., and Ohtomi, M. (2002). Identification of adducin/GTRAP3-18 as a chronic morphine-augmented gene in amygdala. *Neuroreport* 13, 2079–2084.

Kim, J.-H., Lim, Y.-J., Ro, Y.-J., Min, S.-W., Kim, C.-S., Do, S.-H., Kim, Y.-L., and Zuo, Z. (2003). Effects of ethanol on the rat glutamate excitatory amino acid transporter type 3 expressed in *Xenopus* oocytes: role of protein kinase C and phosphatidylinositol 3-kinase. *Alcohol. Clin. Exp. Res.* 27, 1548–1553.

Lander, E.S., Linton, L.M., Birren, B., Nusbaum, C., Zody, M.C., Baldwin, J., Devon, K., Dewar, K., Doyle, M., FitzHugh, W., et al. (2001). Initial sequencing and analysis of the human genome. *Nature* 409, 860–921.

Lee, Y.W., Hennig, B., Fiala, M., Kim, K.S., and Toborek, M. (2001). Cocaine activates redox-regulated transcription factors and induces TNF- α expression in human brain endothelial cells. *Brain Res.* 920, 125–133.

Levenson, J.M., and Sweatt, J.D. (2005). Epigenetic mechanisms in memory formation. *Nat Rev Neurosci* 6, 108–118.

Lim, G., Wang, S., and Mao, J. (2005). cAMP and protein kinase A contribute to the downregulation of spinal glutamate transporters after chronic morphine. *Neurosci. Lett.* 376, 9–13.

Lim, S., Park, M., Jung, H.-K., Park, A.-Y., Kim, D.-I., Kim, J.-C., Bae, C.-S., Kim, K.-Y., Yoon, K.-C., Han, H.J., et al. (2008). Bradykinin stimulates glutamate uptake via both B1R and B2R activation in a human retinal pigment epithelial cells. *Life Sci.* 83, 761–770.

Lin, C.I., Orlov, I., Ruggiero, A.M., Dykes-Hoberg, M., Lee, A., Jackson, M., and Rothstein, J.D. (2001). Modulation of the neuronal glutamate transporter EAAC1 by the interacting protein GTRAP3-18. *Nature* 410, 84–88.

Liu, L., Fu, Y., He, H., Ji, F., Liu, F., and CAO, M. (2011). Expression of EAAT3 in prefrontal cortex and hippocampus in CPP reinstatement rats induced by morphine. *Chinese Journal of Pathophysiology* 27, 1720–1724.

Lowry, O.H., Rosebrough, N.J., Farr, A.L., and Randall, R.J. (1951). Protein measurement with the Folin phenol reagent. *J. Biol. Chem.* 193, 265–275.

Luning Prak, E.T., and Kazazian, H.H. (2000). Mobile elements and the human genome. *Nat Rev Genet* 1, 134–144.

Mao, J., Sung, B., Ji, R.-R., and Lim, G. (2002). Chronic morphine induces downregulation of spinal glutamate transporters: implications in morphine tolerance and abnormal pain sensitivity. *J. Neurosci. Off. J. Soc. Neurosci.* 22, 8312–8323.

Mardikian, P.N., LaRowe, S.D., Hedden, S., Kalivas, P.W., and Malcolm, R.J. (2007). An open-label trial of N-acetylcysteine for the treatment of cocaine dependence: a pilot study. *Prog. Neuropsychopharmacol. Biol. Psychiatry* 31, 389–394.

Maze, I., and Nestler, E.J. (2011). The epigenetic landscape of addiction. *Ann. N. Y. Acad. Sci.* *1216*, 99–113.

Maze, I., Feng, J., Wilkinson, M.B., Sun, H., Shen, L., and Nestler, E.J. (2011). Cocaine dynamically regulates heterochromatin and repetitive element unsilencing in nucleus accumbens. *Proc. Natl. Acad. Sci. U. S. A.* *108*, 3035–3040.

De Meyer, T., Mampaey, E., Vlemmix, M., Denil, S., Trooskens, G., Renard, J.-P., De Keulenaer, S., Dehan, P., Menschaert, G., and Van Criekinge, W. (2013). Quality Evaluation of Methyl Binding Domain Based Kits for Enrichment DNA-Methylation Sequencing. *PLoS ONE* *8*, e59068.

Miller, C.A., Campbell, S.L., and Sweatt, J.D. (2008). DNA methylation and histone acetylation work in concert to regulate memory formation and synaptic plasticity. *Neurobiol. Learn. Mem.* *89*, 599–603.

Moran, L.K., Gutteridge, J.M., and Quinlan, G.J. (2001). Thiols in cellular redox signalling and control. *Curr. Med. Chem.* *8*, 763–772.

Muller, D.L., and Unterwald, E.M. (2004). In vivo regulation of extracellular signal-regulated protein kinase (ERK) and protein kinase B (Akt) phosphorylation by acute and chronic morphine. *J. Pharmacol. Exp. Ther.* *310*, 774–782.

Muratore, C.R., Hodgson, N.W., Trivedi, M.S., Abdolmaleky, H.M., Persico, A.M., Lintas, C., De La Monte, S., and Deth, R.C. (2013). Age-Dependent Decrease and Alternative

Splicing of Methionine Synthase mRNA in Human Cerebral Cortex and an Accelerated Decrease in Autism. *PLoS ONE* 8, e56927.

Nieoullon, A., Canolle, B., Masméjean, F., Guillet, B., Pisano, P., and Lortet, S. (2006). The neuronal excitatory amino acid transporter EAAC1/EAAT3: does it represent a major actor at the brain excitatory synapse? *J. Neurochem.* 98, 1007–1018.

Ohka, F., Natsume, A., Motomura, K., Kishida, Y., Kondo, Y., Abe, T., Nakasu, Y., Namba, H., Wakai, K., Fukui, T., et al. (2011). The Global DNA Methylation Surrogate LINE-1 Methylation Is Correlated with MGMT Promoter Methylation and Is a Better Prognostic Factor for Glioma. *PLoS ONE* 6, e23332.

Powis, G., Briehl, M., and Oblong, J. (1995). Redox signalling and the control of cell growth and death. *Pharmacol. Ther.* 68, 149–173.

Powis, G., Gasdaska, J.R., and Baker, A. (1996). Redox Signaling and the Control of Cell Growth and Death. In *Advances in Pharmacology*, Helmut Sies, ed. (Academic Press), pp. 329–359.

Reichel, C.M., Moussawi, K., Do, P.H., Kalivas, P.W., and See, R.E. (2011). Chronic N-acetylcysteine during abstinence or extinction after cocaine self-administration produces enduring reductions in drug seeking. *J. Pharmacol. Exp. Ther.* 337, 487–493.

Renthal, W., and Nestler, E.J. (2008). Epigenetic mechanisms in drug addiction. *Trends Mol. Med.* 14, 341–350.

Rose, S., Melnyk, S., Pavliv, O., Bai, S., Nick, T.G., Frye, R.E., and James, S.J. (2012). Evidence of oxidative damage and inflammation associated with low glutathione redox status in the autism brain. *Transl. Psychiatry* 2, e134.

Singer, T., McConnell, M.J., Marchetto, M.C.N., Coufal, N.G., and Gage, F.H. (2010). LINE-1 Retrotransposons: Mediators of Somatic Variation in Neuronal Genomes? *Trends Neurosci.* 33, 345–354.

Sun, H., Maze, I., Dietz, D.M., Scobie, K.N., Kennedy, P.J., Damez-Werno, D., Neve, R.L., Zachariou, V., Shen, L., and Nestler, E.J. (2012). Morphine Epigenomically Regulates Behavior through Alterations in Histone H3 Lysine 9 Dimethylation in the Nucleus Accumbens. *J. Neurosci.* 32, 17454–17464.

Trivedi, M.S., and Deth, R.C. (2012). Role of a Redox-Based Methylation Switch in mRNA Life Cycle (Pre- and Post-Transcriptional Maturation) and Protein Turnover: Implications in Neurological Disorders. *Front. Neurosci.* 6.

Ulrey, C.L., Liu, L., Andrews, L.G., and Tollefsbol, T.O. (2005). The impact of metabolism on DNA methylation. *Hum. Mol. Genet.* 14, R139–R147.

Waly, M., Olteanu, H., Banerjee, R., Choi, S.-W., Mason, J.B., Parker, B.S., Sukumar, S., Shim, S., Sharma, A., Benzecry, J.M., et al. (2004). Activation of methionine synthase by insulin-like growth factor-1 and dopamine: a target for neurodevelopmental toxins and thimerosal. *Mol Psychiatry* 9, 358–370.

Waly, M.I., Kharbanda, K.K., and Deth, R.C. (2011). Ethanol Lowers Glutathione in Rat Liver and Brain and Inhibits Methionine Synthase in a Cobalamin-dependent Manner. *Alcohol. Clin. Exp. Res.* 35, 277–283.

Wang, Q., Liu-Chen, L.-Y., and Traynor, J.R. (2009). Differential Modulation of μ - and δ -Opioid Receptor Agonists by Endogenous RGS4 Protein in SH-SY5Y Cells. *J. Biol. Chem.* 284, 18357–18367.

Watabe, M., Aoyama, K., and Nakaki, T. (2008). A dominant role of GTRAP3-18 in neuronal glutathione synthesis. *J. Neurosci. Off. J. Soc. Neurosci.* 28, 9404–9413.

Xu, B., Wang, Z., Li, G., Li, B., Lin, H., Zheng, R., and Zheng, Q. (2006). Heroin-administered mice involved in oxidative stress and exogenous antioxidant-alleviated withdrawal syndrome. *Basic Clin. Pharmacol. Toxicol.* 99, 153–161.

Xu, N.-J., Bao, L., Fan, H.-P., Bao, G.-B., Pu, L., Lu, Y.-J., Wu, C.-F., Zhang, X., and Pei, G. (2003). Morphine withdrawal increases glutamate uptake and surface expression of glutamate transporter GLT1 at hippocampal synapses. *J. Neurosci. Off. J. Soc. Neurosci.* 23, 4775–4784.

Yang, L., Wang, S., Sung, B., Lim, G., and Mao, J. (2008). Morphine induces ubiquitin-proteasome activity and glutamate transporter degradation. *J. Biol. Chem.* 283, 21703–21713.

Yin, D., Woodruff, M., Zhang, Y., Whaley, S., Miao, J., Ferslew, K., Zhao, J., and Stuart, C. (2006). Morphine promotes Jurkat cell apoptosis through pro-apoptotic FADD/P53 and anti-apoptotic PI3K/Akt/NF- κ B pathways. *J. Neuroimmunol.* 174, 101–107.

Yoon, H.-J., Lim, Y.-J., Zuo, Z., Hur, W., and Do, S.-H. (2014). Nicotine decreases the activity of glutamate transporter type 3. *Toxicol. Lett.* 225, 147–152.

Footnotes:

- a) This work was supported by research grants to RD from A2 Corporation Limited and the National Institute for Drug Abuse [R21DA030225]. The content is solely the responsibility of the authors and does not necessarily represent the official views of the National Institutes of Health.
- b) This work has been previously presented at the annual Experimental Biology meeting 2013; Citation - FASEB J. April 2013 27 (Meeting Abstract Supplement) 1180.8.

Link -

http://www.fasebj.org/cgi/content/meeting_abstract/27/1_MeetingAbstracts/1180.8?sid=10f19ee0-a800-4d05-9b2f-cca420fc0a22

- c) Reprints Request would be received by

Richard C. Deth
Northeastern University 148 The Fenway
360 Huntington Avenue
Boston, MA 02115
Telephone: 617-373-4064
FAX: 617-373-8886
Email: r.deth@neu.edu

Figure Legends:

Figure 1: Neuronal redox and methylation pathways. Neurons depend upon cysteine uptake to support GSH synthesis. Cysteine is provided by cleavage of GSH exported by astrocytes, and neurotrophic growth factors promote cysteine uptake via the EAAT3 transporter. (Hodgson et al., 2013) Transsulfuration of homocysteine (HCY) to cysteine is restricted in human brain, increasing reliance upon EAAT3-mediated uptake. Methylation reactions, including DNA methylation, are regulated by methionine synthase, whose activity is dependent upon redox status and GSH levels.

Figure 2: Inhibition of cysteine uptake by morphine via μ -opioid receptors in SH-SY5Y cells. (A) Radiolabeled cysteine uptake by SH-SY5Y human neuroblastoma cells is reduced by increasing concentrations of morphine (0.1 nM to 10 μ M) with an IC_{50} of 2.4 nM. Pretreatment with the non-selective opioid antagonist naltrexone (1 μ M) prevents the morphine-induced decrease of cysteine transport (n = 6); Asterisks (*) indicate a significant difference (p<0.005) from control. (B) SH-SY5Y cells treated with 0.1 μ M morphine showed a pattern of inhibition of cysteine uptake at different time points (0.5, 4 and 24 hrs). Pretreatment with CTAP (0.1 μ M), a specific mu-opioid receptor blocker, abrogated the effects of morphine. Pre-treatment with naltrindole (NTI, 0.1 μ M), a specific δ -opioid receptor blocker, did not inhibit the effects of morphine on cysteine uptake (n=6). Asterisks (*) indicates a significant difference (p<0.05) from no treatment control. Grey bar represents no treatment control (NTC). Non-specific binding was subtracted from total cysteine uptake.

Figure 3: Differential involvement of G-proteins and downstream signaling kinases in morphine-induced inhibition of cysteine uptake by SH-SY5Y cells. (A) Short-term (0.5 and 4 hours) morphine treatment (0.1 μM) inhibited cysteine uptake by SH-SY5Y human neuroblastoma cells, and this effect was blocked by pretreatment with pertussis toxin, a $G_{i/o}$ inhibitor (PTX, 0.5 $\mu\text{g/mL}$, 24 hrs), but not by cholera toxin, a G_s inhibitor (CTX, 0.5 $\mu\text{g/mL}$, 24 hrs) (n=6). Long-term (24 hr) morphine treatment (0.1 μM) induced inhibition of cysteine uptake that was blocked by pretreatment with cholera toxin, but not pertussis toxin. (B) The short-term (4 hrs) inhibitory effect of morphine on cysteine uptake was blocked by pretreatment with the PKA inhibitor H-89 (0.1 μM) (n=6). The long-term (24-hours) effect of morphine (0.1 μM) on cysteine uptake was blocked by pretreatment with the MEKK inhibitor PD98059 (10 μM) (n=6). Asterisks (*) show a significant difference ($p < 0.005$) from no-treatment control (NTC, grey bar).

Figure 4. Effect of morphine on cellular cysteine concentration and GSH/GSSG and SAM/SAH ratios in SH-SY5Y cells. Intracellular cysteine, GSH/GSSG and SAM/SAH ratios were decreased by morphine treatment at (A) 4 hours and (B) 24 hours. Pre-treatment with the PKA inhibitor H-89 (0.1 μM) blocked the effects of morphine (0.1 μM) at 4 hours and the MEKK inhibitor PD98059 (10 μM) blocked the effects of morphine at 24 hours (n=4). Asterisks (*) indicate a significant difference ($p < 0.05$) from untreated control values.

Figure 5: Effect of morphine on global DNA methylation in SH-SY5Y cells. Cells were treated with morphine (0.1 μ M) for 4 hours and 24 hours in presence or absence of H-89 (0.1 μ M) and PD98059 (10 μ M) respectively (n=6). Global methylation was quantified using an anti-5-methylcytosine antibody, measured by ELISA assay. No significant changes were observed after 4 hours of morphine treatment, but 24 hours of morphine treatment induced significant hypomethylation. Asterisks (*) indicate a significant difference ($p < 0.05$) from untreated controls.

Figure 6: Morphine induces hypomethylation in LINE-1 repetitive elements and increases LINE-1 mRNA levels. (A) Morphine (0.1 μ M) induced changes in site-specific methylation content for individual CpG sites on promoter regions of LINE-1 HS family, as determined by bisulfite conversion and pyrosequencing. Pos1-4 indicates individual CpG sites, normalized against control values. Asterisk (*) indicates significant difference ($p < 0.05$) compared to control; Double asterisks (**) indicate $p < 0.01$ compared to control. (B) Promoter methylation (TSS \pm 500 base pairs) of LINE-1. Morphine increased promoter methylation after 4 hours, which returned to normal levels after 24 hours of morphine treatment; N=5. (C) qRT-PCR analysis of LINE-1 mRNA levels. 4 hours of morphine treatment decreased LINE-1 mRNA levels, whereas 24 hours of morphine treatment induced a large increase. Pretreatment with H-89 or PD98059 blocked the changes in LINE-1 mRNA levels after 4 or 24 hours of morphine treatment, respectively. Asterisks (*) indicate a significant difference ($p < 0.05$) from untreated controls.

Figure 7: Proposed mechanism. In SH-SY5Y cells, morphine inhibition of EAAT3 via the μ -opioid receptor is mediated by MAPK and PKA signaling via $G\alpha_{i/o}$ and $G\alpha_s$. Activation of the μ -opioid receptor can also lead to GTRAP3-18 activation (Ikemoto et al., 2002; Lin et al., 2001), which reduces the level of EAAT3 surface expression. PKA pathways can activate transcriptional factors like CREB, but can also activate the PTEN/ubiquitin/Nedd4 pathway, which promotes degradation of EAAT3. Further, the PKA and ERK pathway can also mediate phosphorylation of EAAT3, which can affect surface expression and/or EAAT3 activity directly. Thus, morphine treatment reduces GSH/GSSG and SAM/SAH ratios, leading to epigenetic changes subsequently affecting transcription.

Figure 1

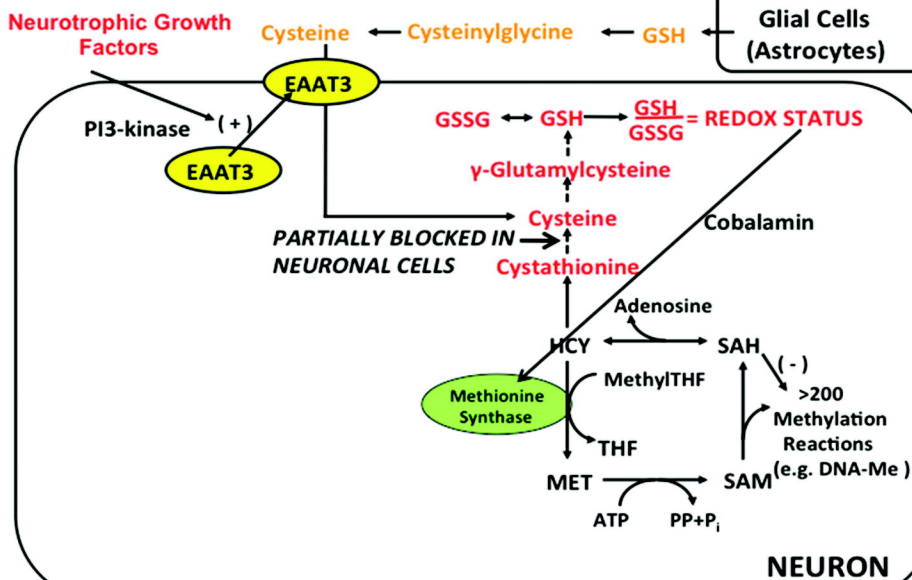
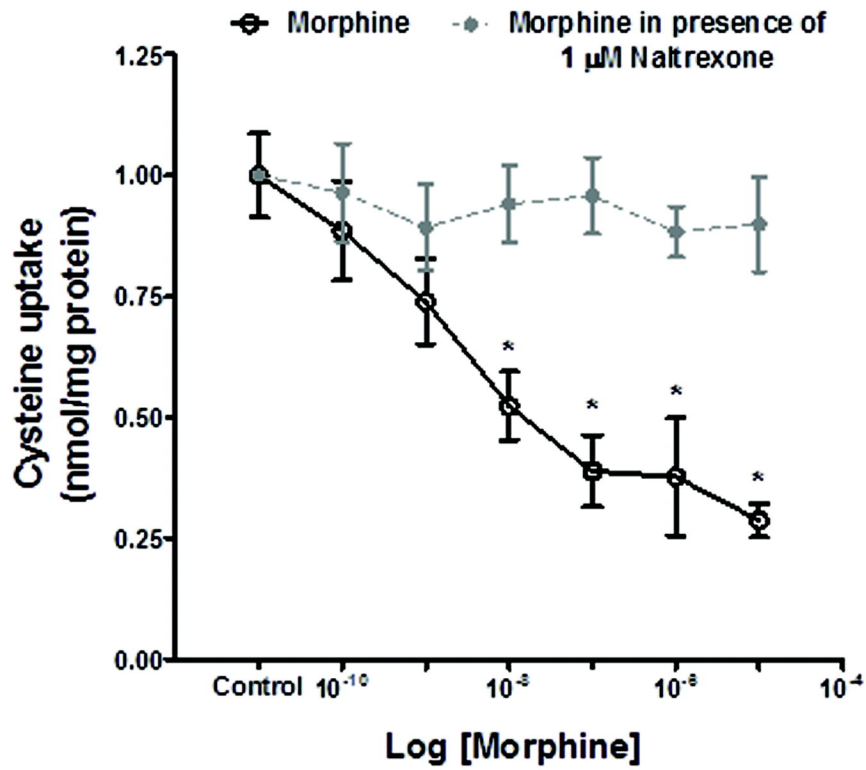
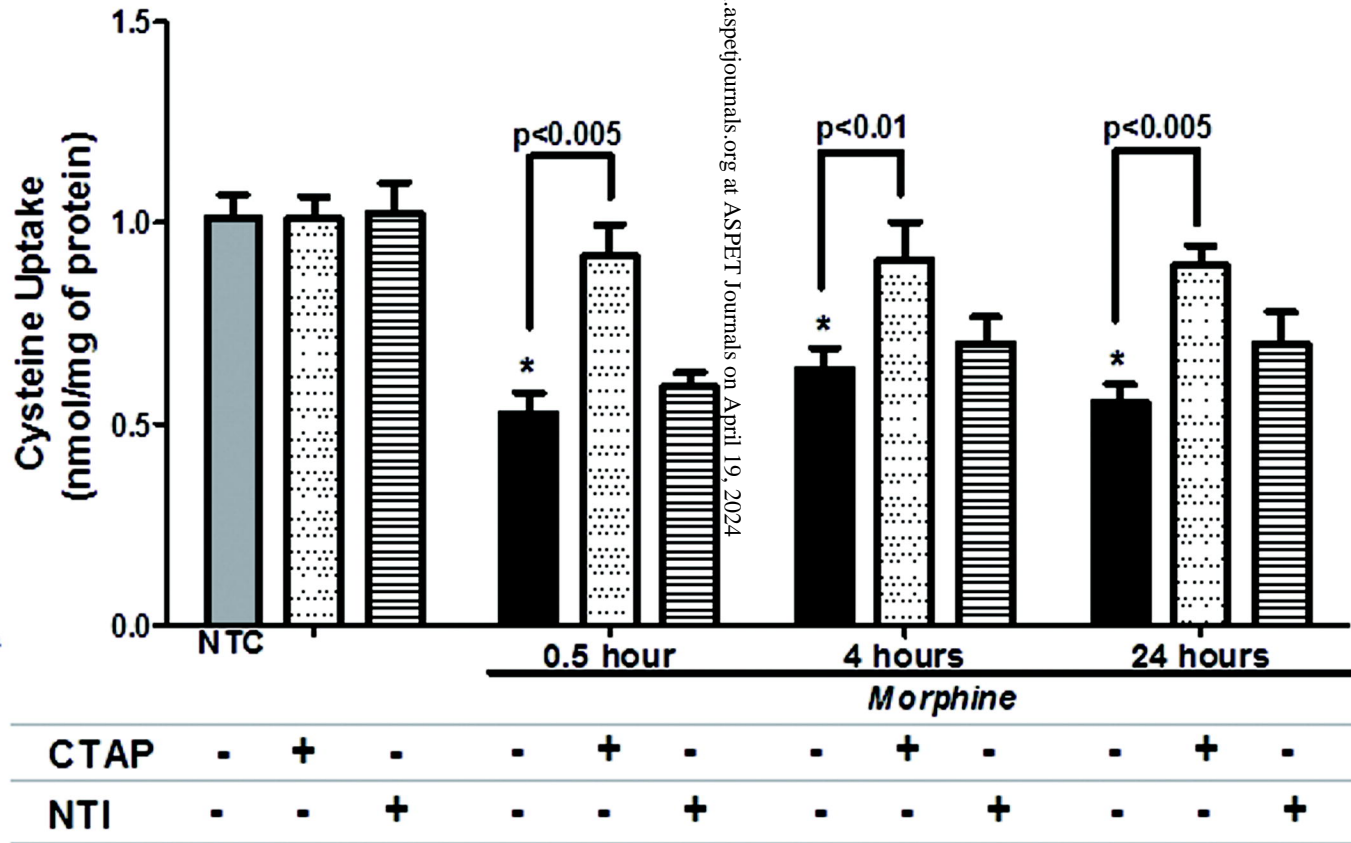


Figure 2

A.



B.

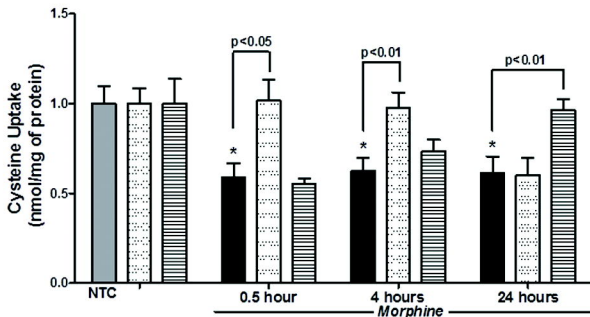


Downloaded from molpharm.aspetjournals.org at ASPET Journals on April 19, 2024

CTAP	-	+	-	-	+	-	-	+	-	-	+	-
NTI	-	-	+	-	-	+	-	-	+	-	-	+

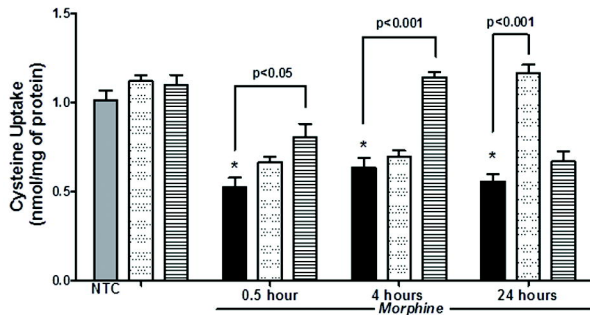
Figure 3

A.



pertussis toxin	-	+	-	-	+	-	-	+	-	-	+	-
cholera toxin	-	-	+	-	-	+	-	-	+	-	-	+

B.



PD98059	-	+	-	-	+	-	-	+	-	-	+	-
H89	-	-	+	-	-	+	-	-	+	-	-	+

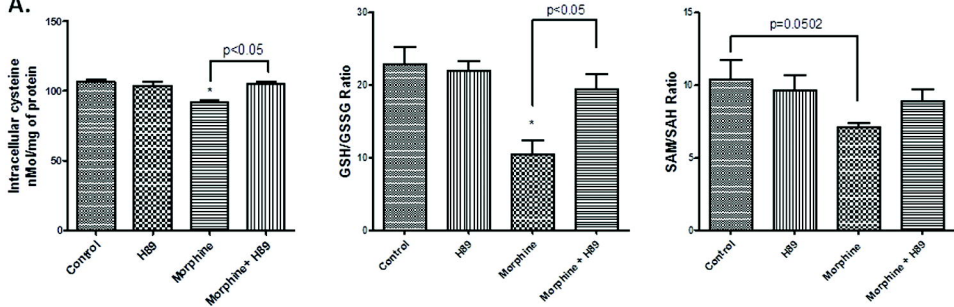
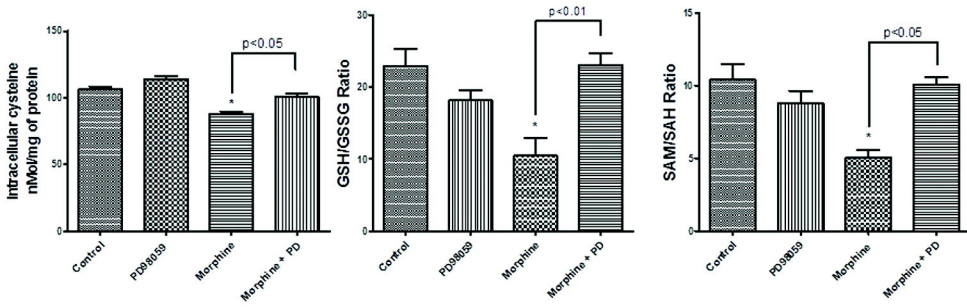
Figure 4**A.****B.**

Figure 5

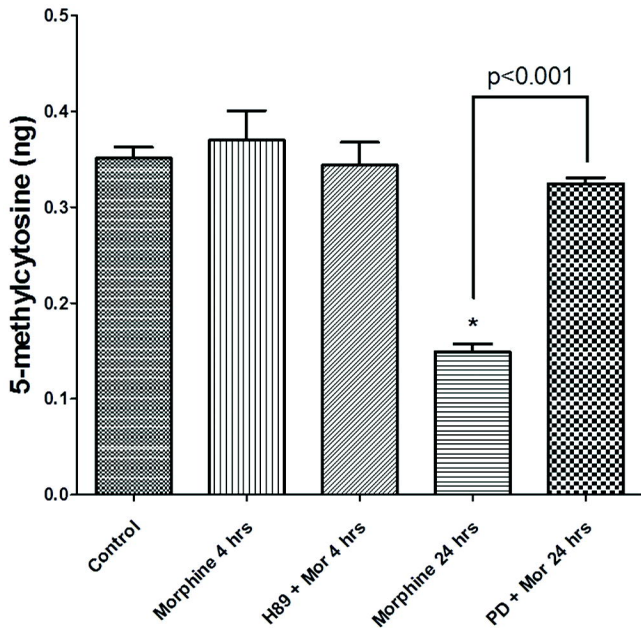


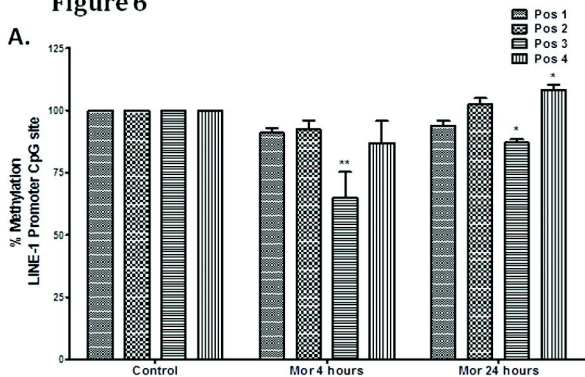
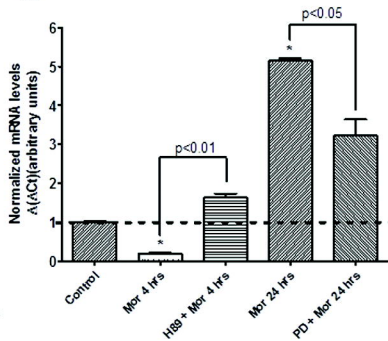
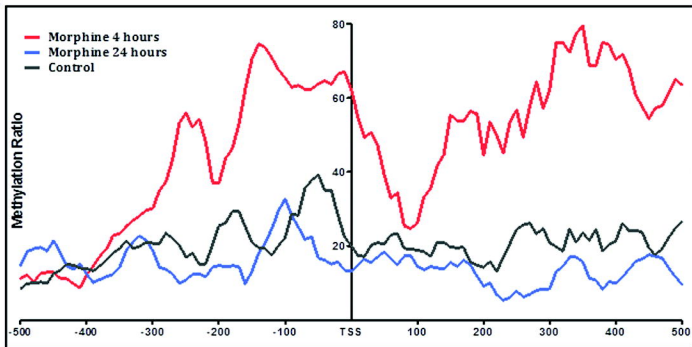
Figure 6**A.****C.****B.**

Figure 7

